# ON THE ISSUE OF ANALYSIS OF ACOUSTIC EMISSION EVENT STATISTIC ON DATA OF SINGLE SENSOR IN ROCK THERMAL FRACTURE EXPERIMENTS

P.A. Kaznacheev[1], Z.-Yu.Ya. Maibuk[1], A.V. Ponomarev[1],
V.B. Smirnov[1, 2], N.B. Bondarenko[1, 2]

[1] *Schmidt Institute of Physics of the Earth, Russian Academy of Sciences, Moscow, Russia*
[2] *Lomonosov Moscow State University, Moscow, Russia*

**Abstract**. Authors examine the problem of estimation of b-value for energy distribution of thermal acoustic emission (TAE) events on basis of amplitude distribution of TAE impulses. Impulses are registered by single TAE sensor. Authors have analyzed the effect of factors, associated with elastic waves propagation, on the energy of impulses. The analysis shows, that effect of elastic waves absorption in heated sample is the most significant from these factors. Two events of energy distribution are considered – with one and two sub-functions. It has shown, that the same b-value of registered impulse amplitude distribution and initial event distribution is observed if only b-value is stable in all TAE-event energy range (one sub-function). In this situation, there is one characteristic generation mechanism of events in all sample volume. But if b-value is not stable in different energy ranges (two sub-functions), then elastic waves absorption in the sample distorts initial distribution. Authors propose technique of "true" b-value estimation on basis of distribution analysis of registered TAE impulses in several amplitude subranges.

**Keywords:** thermally stimulated rock failure, thermoacoustic emission, b-value, absorption of elastic waves.

## Introduction

In some laboratory experiments of rock failure, one or several sensors are used for registration of acoustic emission (AE) that is not enough for location and determination of the energy of AE-events. Events of acoustic emission are individual acts of microfracturing – formation and growth of microcracks, intergranular sliding, explosions of gas liquid inclusions, lattice rearrangement, etc., that are accompanied by energy emission in the form of generation of the elastic wave packet (acoustic emission impulse). Note that the very notions of "event" and "impulse" of acoustic emission are unique only in the case of its discreteness when individual impulses and events are distinguished in the flow of impulses and events. Impulses from AE-events reach the sensors through the medium. In the statistical analysis of parameters of stream of AE-impulses recorded by the sensors, arises the question of how to estimate *b-value*[1] and other statistical parameters of the stream of AE-events. When elastic waves propagate from the AE-events, we can observe their spreading, absorption, refraction, re-reflection and interference. If during the experiment the quantitative characteristics of these processes change, then the parameters of the registered impulse flow also change. Data of the ultrasonic sounding show that absorption of the elastic waves can increase by several orders, especially during thermally stimulated rock failure [*Vasin et al.,* 2006]. Therefore, the competent question is how these processes influence the parameters of the recorded stream of AE-impulses.

---

[1] The name of the parameter adopted in the English literature; further we will use *b.*

In our laboratory experiments on the study of thermally stimulated rock failure [*Kaznacheev et al.,* 2017], a single thermoacoustic emission (TAE) sensor is used – a sensor of integrated acoustics (Fig. 1).

**Fig. 1.** The laboratory setup for thermoacoustic emission study: the cross-sectional view. *1* – test cylindrical rock sample; *2* – support; *3* – cylindrical acoustic waveguide; *4* – furnace body; *5* – sensor of integral acoustic emission; *6* – heating element; *7* – schematic symbol of thermal radiation; *8* – layer of indium. Dimensions are given in millimeters
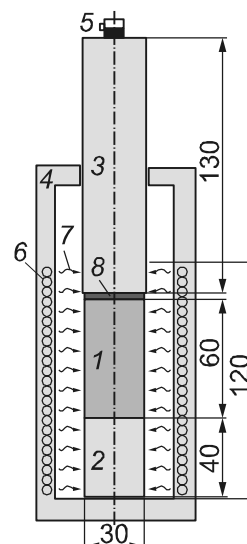


To the end of the test cylindrical sample through the indium layer is attached a cylindrical acoustic waveguide. TAE sensor is placed on its other end. With the aid of *A-Line* 32*D* recording system, the parameters of the TAE impulses are determined – amplitude, impulse rise time, duration, etc., on which basis can be determined statistics of impulse stream – distribution of their number by amplitudes, etc. Energy distribution of the number of TAE events in the sample is certainly associated with the amplitude distribution of the number of impulses, but cannot be definitely reconstructed using a single sensor. There is a problem of estimating statistical parameters of the stream of TAE events according to the data on TAE impulse stream, which solution is necessary for analyzing the nature of fracture growth over time (by *b* parameter and etc.) and for identifying different mechanisms of TAE generation. For example, thermoacoustic emission can be caused both by the temperature and its gradient [*Shkuratnik, Voznesenskij, Vinnikov,* 2015], that we observe in TAE activity variations [*Kaznacheev et al.,* 2017]. Each of mechanisms probably has its own law of energy distribution of events and, therefore, its own value of parameter *b*.

When solving the given research problem, it is necessary to take into account the initial «true» law of the energy distribution of events; absorption, divergence, refraction and interference of elastic waves; direction of energy emission from TAE events.

First, a theoretical analysis of influence of above noted factors on the recorded TAE impulse distribution was carried out. Then, the associated features of TAE impulse distribution were identified and an estimation method for statistical parameters of TAE events stream was proposed.

**Factors affecting the character of distribution of thermoacoustic emission impulses**

*The law of energy distribution of events*

The law of energy distribution of acoustic emission events during the rock fracturing can have a different character depending on the type of developing defects, their distribution by characteristic sizes, on the very nature of fracture growth. The most commonly considered

are power-series, exponential and gamma distributions [*Ponomarev et al.,* 1997; *Vettegren et al.,* 2005; *Damaskinskaya,* 2018]. The first two differ in monotonously decreasing character and have only two parameters, so they are widely used for the analysis of statistics of acoustic emission events [*Vettegren et al.,* 2004; *Damaskinskaya et al.,* 2017]. Their use is valid only in the case when for the given laboratory sensitivity AE impulses from strong events are recorded, composing tail of complex distribution. This tail can also be represented by exponential or power law.

Assume that the fundamental law of energy distribution of acoustic emission events is similar to the Guttenberg-Richter power law for seismic events [*Ponomarev et al.,* 1997], that looks like

$$\lg N_E = a' - b \lg E ,$$ (1)

where $N_E$ is a number of events with energies in the range $[E, E+dE]$; $a'$ and $b$ are parameters of approximation. When registering an acoustic impulse, it's amplitude that is determined, and not its impulse energy. Each event with energy $E$ can be attributed to some "true" amplitude of the acoustic impulse and take

$$E = k_p A^2 ,$$ (2)

where $k_p$ is a proportionality coefficient. This is true only on assumption of a small change in the shape of acoustic impulse during propagating. Note that in acoustic emission recording systems (*ALine* 32D type) the acoustic impulse energy is estimated using different algorithms, but in the most common version it is assumed to be proportional to the square of the maximum amplitude [AE Test, 2017]. Therefore, by $A$ we mean the maximum amplitude of the acoustic impulse – both "true" and recorded. In such case from (2) it follows that

$$\lg E = \lg k_p + 2 \lg A .$$

Further, we will express the energy and amplitude in decibels (dB) relative to 1 J and 1 μV, respectively:

$$E\,[\text{dB}] = 10 \lg k_p + A\,[\text{dB}] .$$ (3)

Combining (1) and (3), we proceed to the distribution law of events expressed for "true" amplitudes of acoustic impulses in the form

$$\lg N_A = a - bA ,$$ (4)

where $N_A$ is a number of events with amplitudes in the range $[A, A+dA]$; value $a$ takes into account $a'$ and $\lg k_p$.

In addition to the noted distribution law (one sub-function) there can be others, more complex laws under the action of different generation mechanisms of seismic events [*Okal, Romanowicz,* 1994; *Amitrano,* 2012]. Efforts of seismologists are currently focused on clarification of distribution nature at different magnitude intervals [*Pisarenko, Rodkin,* 2017]. In the simplest case, representation of complex distributions is reduced to piecewise-linear approximation by a law as in (4).

We confine ourselves to the case when the distribution law is approximated by (4) with different parameters for two adjacent amplitude ranges (two sub-functions):

$$\lg N_A = \begin{cases} a_{low} - b_{low} A, \ at \ A \leq A_{thold}, \\ \\ a_{high} - b_{high} A, \ at \ A \geq A_{thold}, \end{cases}$$ (5)

where $a_{low}$, $b_{low}$, $a_{high}$, $b_{high}$ are parameters of approximation for two amplitude ranges; $A_{thold.}$ is a threshold amplitude where distribution law changes. The considered variants of distribution law are shown in Fig. 2.
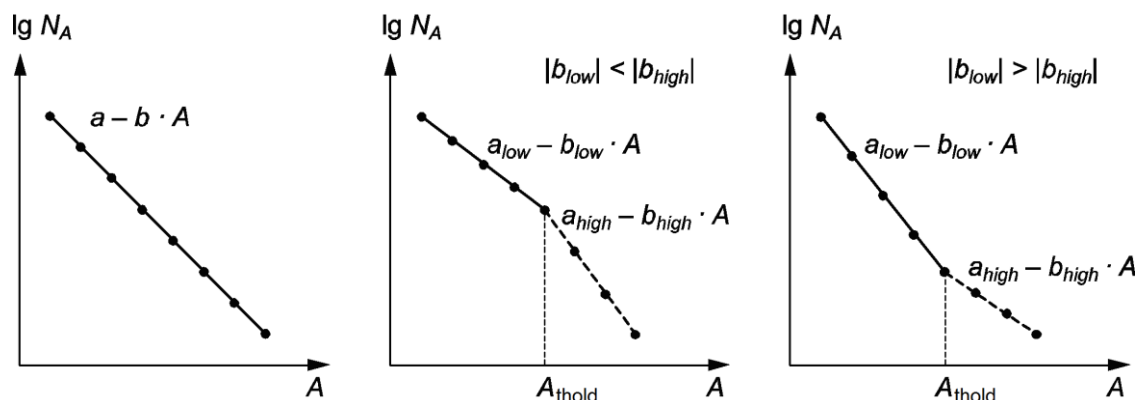


**Fig. 2.** The considered variants of AE-events energy distribution: the single describing function on (4) (left), and the piecewise continuous describing function from two sub-function on (5) (two versions – center and right)

As it was noted above, with thermally stimulated fracturing, the complex distribution law can be associated with the initiation of TAE by temperature and its gradient. Besides, it may be associated with the distribution inhomogeneity of TAE events over the sample volume in the radial direction, since the increase in activity of microfracturing growth occurs first in its outer layers, as they warm up earlier. Further, we assume that along the sample axis any mechanisms act homogeneously.

*Acoustic wave attenuation on the way to the receiver*

When propagating from a source, the acoustic wave spreads and loses energy due to the absorption by the medium. Let us estimate the influence of spreading and absorption, assuming that all AE sources are concentrated in the sample and not in the waveguide and not in the elements of the heating device. This is confirmed by test experiments without a sample and the correlation of TAE activity with heating [*Kaznacheev et al.,* 2017].

For the case of spherical acoustic wave propagating in space from the AE event with energy $E$, it is possible to determine the energy flux density of wave $p$:

$$p = \frac{E_{ds}}{ds} = \frac{E}{4\pi r^2} = \frac{p_\Omega}{r^2}, \tag{6}$$

where $E_{ds} = Ed\Omega/4\pi$ is the energy falling on small area $ds$ at the registration point; $d\Omega = ds/r^2$ is a solid angle under which $ds$ area is visible from the event spot; $r$ is a distance from the AE event to the registration point; $p_\Omega = E/4\pi$ is an energy flux density of spherical wave per unit of solid angle. We operate with the energy flux density $p$ (dimension J/m$^2$) instead of intensity $I$ (dimension W/m$^2$ = J/(s·m$^2$)), since from the AE event propagates not a monochromatic acoustic wave, but a wave packet – acoustic impulse which energy is assumed to be proportional to the square of the maximum amplitude of impulse $A$.

Energy of the acoustic impulse recorded by the acoustic emission sensor (AES) denoted as $E_{AES}$, is equal to:

$$E_{AES} = pS_{AES} \cos(\varphi) \tag{7}$$

where $S_{\text{AES}} \approx \pi R^2_{\text{AES}}$ is an effective area of sensitive element of the AE sensor (see Fig. 1) with the radius of sensitive element of the used common AE sensor $R_{\text{AES}} \approx 0.0065$ m; $\varphi$ is an angle between normal to the $S_{\text{AES}}$ site and direction of wave propagation. Taking into account (6) we obtain

$$E_{\text{AES}} = \frac{p_\Omega}{r^2} \pi R^2_{\text{AES}} \cos(\varphi) \,. \tag{8}$$

Let us determine the impulse energy taking into account its absorption in the sample and waveguide. In the linear absorption models, it is assumed that absorbed energy is directly proportional to the wave energy. The wave loses its energy at the distance $r$ in its propagation direction in the absorbing medium according to the formula

$$p_B = p_A \cdot 10^{-Dr} \,, \tag{9}$$

where $p_A$ and $p_B$ is energy flux density of the wave at the points $A$ and $B$, respectively; $D$ is a specific absorption coefficient of acoustic energy by the medium (dimension 1/m). For the plane wave under $p_A$ and $p_B$ should be understood the energy flux density per unit of area, for the spherical wave – energy flux density per unit of solid angle. The expression of absorption coefficient $k_{att}$ in dB/m is characteristic for acoustic systems of nondestructive testing – $k_{att}=10 \cdot D$. Based on the fact that we work in the narrow frequency range (150–500 kHz for *ALine* 32D together with AE sensor) and, assuming that the spectral composition of TAE acoustic impulses (microcracks scale) does not change greatly during the experiment, we will consider the absorption coefficient as frequency independent.

The $k_{att}$ value depends both on the sample material and the temperature. Results of experiments performed by different authors who investigated thermally stimulated failures clearly demonstrate the change in the absorption properties of the medium during heating. These changes can be quantitatively evaluated, for example, by the results of experiment given in [*Vasin et al.,* 2006]. Authors of this work, with slow heating of marble, observed the energy decrease of elastic waves of through sounding by more than 25 times during the entire heating. Sounding base was about 0.03 m in size, i.e. absorption increment was ~450 dB/m. Taking into account the above, we took the specific absorption coefficient range of the sample material $k_{att}$ from 100 to 1000 dB/m.

*Refraction, reflection, interference of elastic waves*
*and radiation directivity from the acoustic emission event*

Subtitled factors are essential for estimating the impulse energy and require a separate study. It is impossible to consider their influence according to the data of one AE sensor. But with a large ratio of the rod length to its diameter (from 4–5 and more [*Davies,* 1961]), it can be assumed that the wave pattern of AE impulse in the cross-section of the rod is close to the wave pattern of elastic wave propagation in infinite rods. The noted is true in our case, since the ratio of the length to diameter of only one waveguide is >6. In addition, we assume that the impulse energy is proportional to the square of its maximum amplitude that usually corresponds to one of the first (1–5) half-waves. In such case, we can neglect the influence of interference of the wave, since the beginning of the impulse corresponds to its head part and does not have time to be distorted by interference. Note, that determination of radiation directivity, even of the Hsu-Nielsen sources, used for calibration of acoustic emission monitoring systems is a topic for individual studies (see, for example, [*Markov,* 2007; *Sych,* 2016]). Therefore, we assume that impulse energy from events of different directions remains proportional to the

square of its maximum amplitude and its attenuation is influenced only by divergence and absorption.

*Evaluation of influence of attenuation factors*

The complete expression for the acoustic impulse energy recorded by the sensor ($E_{AES}$), and for the event energy ($E$) taking into account the divergence (8) and absorption (9) can be written in the form:

$$E_{AES} = E \frac{\cos(\varphi)}{4\pi r^2} \cdot 10^{-D_s r_s} \cdot 10^{-D_g r_g} R_{AES}^2,$$

where $D_s$ and $D_g$ are specific absorption coefficients for the material of the sample and the waveguide; $r_s$ and $r_g$ are distances traveled by the impulse in the sample and the waveguide; $r = r_s + r_g$ is a distance from the event to AE sensor. We represent the ratio of $E_{AES}$ to $E$ in a logarithmic view with a dimension dB and highlight characteristic components

$$K_\Sigma = 10\lg \frac{E_{AES}}{E} = -K_I(\varphi) - K_{II}(r) - K_{III}(r_s) - K_{IV}(r_g) + C_1, \qquad (10)$$

$$K_I(\varphi) = 10\lg \frac{1}{\cos\varphi}, \qquad (11)$$

$$K_{II}(r) = 10\lg(4r^2), \qquad (12)$$

$$K_{III}(r_s) = k_{att1} r_s, \qquad (13)$$

$$K_{IV}(r_g) = k_{att2} r_g, \qquad (14)$$

where $K_\Sigma$ is a final coefficient of "attenuation" of the event energy; $K_I - K_{IV}$ are the "attenuation" coefficients of the event energy only due to the slope between the direction of the wave propagation and sample axis ($K_I$), only due to the wave spreading ($K_{II}$), only due to the wave absorption in the sample ($K_{III}$), only due to the wave absorption in the waveguide ($K_{IV}$); $C_1$ is a constant depending only on AE sensor parameters; $k_{att1}$ and $k_{att2}$ are specific absorption coefficients in the material of the sample and the waveguide, respectively.

Let us estimate the spread in the coefficients for different positions of AE event in the sample. For that purpose, we select four characteristic points on the setup scheme (Fig. 3, numbers in circles) and calculate for them the values of the signal attenuation coefficients (Table).
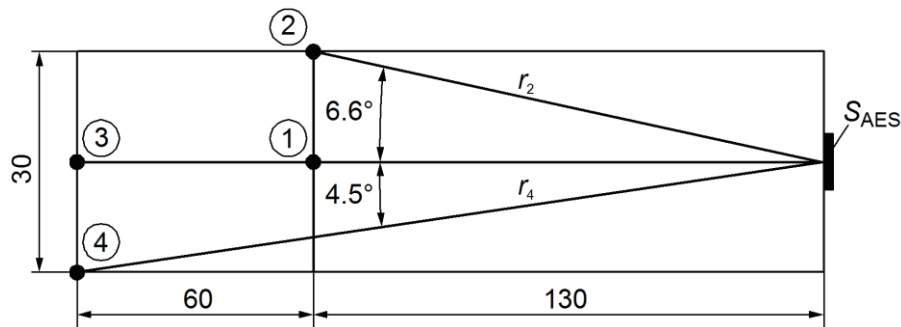


**Fig. 3.** The scheme of the laboratory setup (see Fig. 1), used for calculation of the effect of elastic wave spreading and absorption. Numerals in circles are numbers of the selected characteristic points; $r$ – distance from AE event to AE sensor; $S_{AES}$ – effective area of detector element of AE sensor. Dimensions are given in millimeters

Values of signal attenuation coefficients
for the selected characteristic points 1–4

| Point | Distance from the event to AE sensor $r$, m | Angle between the setup axis and the direction to AE sensor $\varphi$, ° | Attenuation coefficient $K$, dB | | | |
|-------|------|------|-------|-------|-------|-------|
| | | | $K_{\mathrm{I}}$ | $K_{\mathrm{II}}$ | $K_{\mathrm{III}}$ | $K_{\mathrm{IV}}$ |
| 1 | 0.130 | 0 | 0 | −11.7 | 0 | $0.13 \cdot k_{att2}$ |
| 2 | 0.129 | 6.58 | 0.029 | −11.8 | 0 | $0.13 \cdot k_{att2}$ |
| 3 | 0.190 | 0 | 0 | −8.4 | 6–60 | $0.13 \cdot k_{att2}$ |
| 4 | 0.189 | 4.51 | 0.013 | −8.4 | 6–60 | $0.13 \cdot k_{att2}$ |

Since the $K_{\mathrm{I}}$ coefficient is small compared to the other coefficients, it can be neglected; $K_{\mathrm{IV}}$ is almost the same for all event positions. $K_{\mathrm{II}}$ varies from −11.8 to −8.4 dB, i.e. the total change in this coefficient is about 3.4 dB. Negative value of $K_{\mathrm{II}}$ is associated with the fact that formally according to (12) we determine the spreading wave attenuation due to the spreading compared to the wave energy at a unit distance (i.e. at $r=1$ m). $K_{\mathrm{III}}$ varies in the range from 0 to 6–60 dB, i.e. its total change is 6–60 dB and is crucial for $K_\Sigma$. Moreover, $K_{\mathrm{II}}$ also almost linearly depends on the distance $r_s$, traveled by the wave in the sample ($r_s < r_g/2 \approx \mathrm{const} < 1$):

$$K_{\mathrm{II}}(r) = 10 \lg(4r^2) = 20 \lg(2(r_s + r_g)) \propto r_s,$$

therefore spreading can be taken into account by a simple addition to $k_{att1}$ − specific absorption coefficient in the sample. In our case (see Fig. 1) addition to $k_{att1}$ for the linear approximation $K_{\mathrm{II}}$ will be about 60 dB/m.

Thus, when analyzing the statistics for estimating the energy attenuation of the acoustic impulse depending on the distance $r_s$, traveled by the impulse in the sample we can be guided by the formula (13).

### Amplitude distribution of impulses

Further we consider how the energy distribution law of AE events and attenuation affect the amplitude distribution of the impulses. In Fig. 4 is given the implementation of the model for the one sub-function law of the energy distribution of events that we will use for the analysis. Function describing $\lg N$, was determined depending on two variables − distance $z$ along the sample axis from the sample-waveguide contact to the event place ($z=0$ m at the sample-waveguide contact and $z=h=0.06$ m at the far end of the sample) and the registered amplitude $A_{\mathrm{reg.}}$ of the acoustic impulse ($A_{\mathrm{reg.}}$ is given in dB in the range from $A_{\min}$ to $A_{\max}$). There are no upper and lower limits along the $\lg N$ axis, since the calculation determines the normalized value of $N$, but for clarity, we can consider $\lg N=0$ (i.e. $N=1$) in the intersection point of the axes.
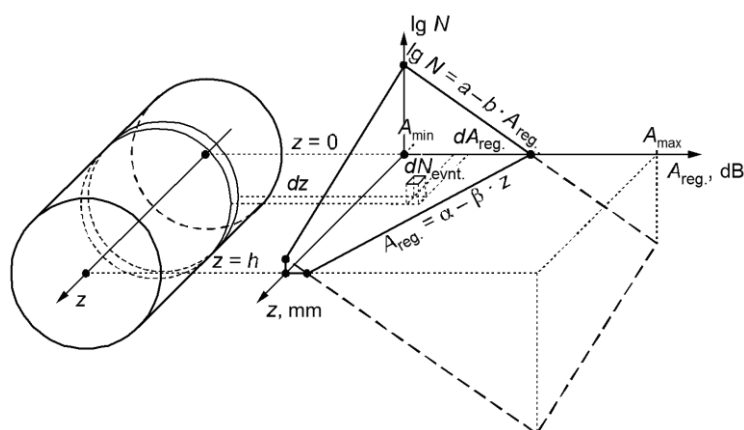
**Fig. 4.** The model for determining the amplitude distribution of AE-impulses. See text for explanations

Dependence of lg$N$ on $A_{\text{reg.}}$ in the plane $z=0$ is determined by the selected initial energy distribution law of the events and, respectively, by "true" amplitudes $A$, as there is no attenuation in the sample at $z=0$. Dependence of $A_{\text{reg.}}$ on $z$ in the plane lg$N=0$ is defined by the attenuation law of amplitude of the event. In a visual representation it determines the maximum amplitude that events with smaller amplitude will be registered ($N \geq 1$) for, in accordance with (13):

$$A_{\text{reg.}} = \alpha - \beta z,\qquad(15)$$

where $\alpha = A$ is a "true" amplitude of the event; $\beta$ is an attenuation rate.

We divide the entire sample along the axis into thin layers $dz$, and the amplitude range $[A_{\min}, A_{\max}]$ into elementary intervals $dA_{\text{reg.}}$. A number of events is $dN_{\text{evnt.}}$ in each considered "cell". $dN_{\text{evnt.}}$ will be registered by a sensor is determined by the function $f(A_{\text{reg.}}, z)$, that describes the event density distribution depending on $A_{\text{reg.}}$, $z$, distribution law and attenuation. For the one sub-function law of distribution from (4) and (15) we have

$$f(A_{\text{reg.}}, z) = 10^{a - bA_{\text{reg.}} - b\beta z}.\qquad(16)$$

To find the number of registered impulses with amplitudes $[A_{\text{reg.}}, A_{\text{reg.}} + dA_{\text{reg.}}]$, it is necessary to determine the number of events that give impulses of the specified amplitudes in the entire volume of the sample. This is accomplished by the integration for each $dA_{\text{reg.}}$ at the given $A_{\text{reg.}}$ over all $dz$ from $z=0$ to $z=h$. Then the number of registered impulses $dN$ in this layer of amplitudes $dA_{\text{reg.}}$ is determined as

$$dN = dA_{\text{reg.}} \int_{0}^{h} f(A_{\text{reg.}}, z)dz.\qquad(17)$$

Amplitude distribution law of impulses will be sought in the form normalized to the maximum $dN$, that, apparently, is achieved at $A_{\min}$. In this case a relative number of impulses $n$ with the current recorded amplitude $A_i$ is determined as

$$n = \frac{dN_{A_i}}{dN_{A_{\min}}} = \frac{dA_{\text{reg.}} \int_{0}^{h} f(A_i, z)dz}{dA_{\text{reg.}} \int_{0}^{h} f(A_{\min}, z)dz}.\qquad(18)$$

Omitting the intermediate calculations, for the one sub-function distribution law we get

$$n = 10^{-b(A_i - A_{\min})}.\qquad(19)$$

For the two sub-function law the formula representation is lengthy, so we write

$$n = n(A_i, A_{\min}, A_{\text{thold}}, \beta, b_{\text{low}}, b_{\text{high}}). \tag{20}$$

Thus, according to (19) the attenuation does not affect the amplitude distribution of the impulses at the one sub-function energy distribution law of the initial events. For the two sub-function law the dependence is more complicated and in certain amplitude range the attenuation effect obviously takes place (Fig. 5).

Attenuation significantly distorts the picture as compared to the "true" distribution. At the same time, the two sub-function nature of distribution itself is visually lost and the threshold amplitude is not determined. The distortion occurs already at relatively small attenuation of about 100 dB/m. However, there are subranges of small and large amplitudes where the slope of impulse distribution plot is close the initial slope of the event distribution plot.

In connection with the noted, an experimental method for analyzing the distribution of impulses was proposed. It allows to judge the event distribution type. To distinguish between one and two sub-function laws, we can separately determine the b-value of impulses at least in two adjacent amplitude subranges. In the example given above in Fig. 5, such subranges are 36–41 and 41–46 dB, where even with a small attenuation can be seen the difference between slopes of the curves. It leads to the conclusion that the nature of the energy distribution of events is more complex than one sub-function.
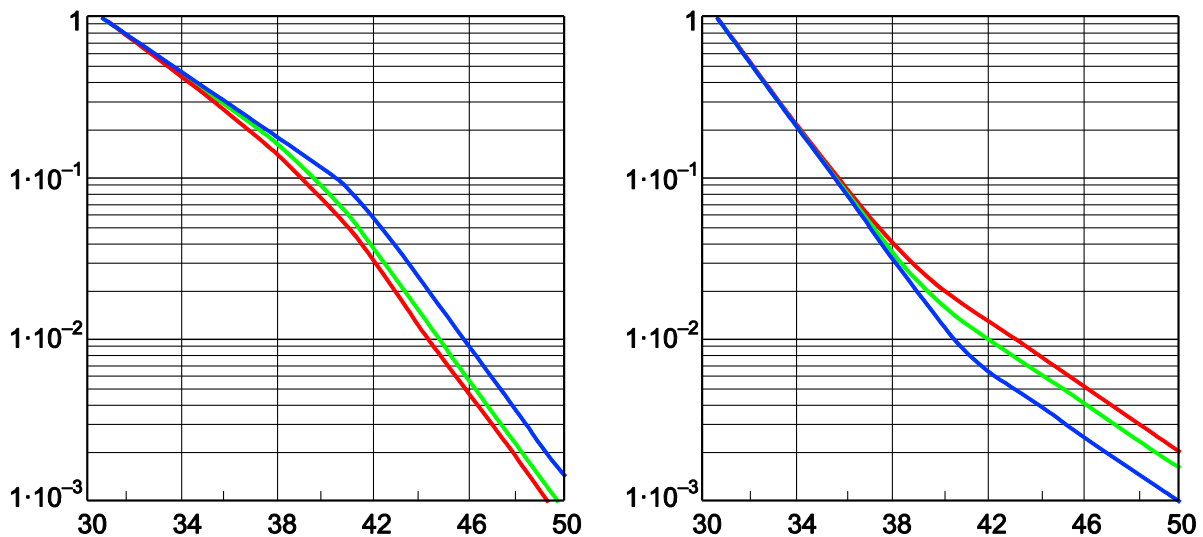


**Fig. 5.** An example of distribution of relative number of AE-impulses by amplitudes, for law of AE-events energy distribution described piecewise function: for $b_{low} < b_{high}$ (left) and for $b_{low} > b_{high}$ (right), the threshold amplitude for sub-functions is 41 dB (see Fig. 2). Blue, green and red curves are given for the attenuation of 0, 100 and 1000 dB/m, respectively. Each of the curves is normalized to its maximum value

The lack of difference in slopes indicates either one sub-function distribution law or the fact that subranges are chosen away from the threshold amplitude in two sub-function law. In such case it is necessary to determine the slope over the wider amplitude range.

The proposed method can be applied both in the sliding time window and for individual characteristic stages of experiments involving various mechanisms of generation of events. A correct estimate of the slope requires a controlled sufficient number of impulses with the maximum analyzed amplitude.

Currently, the authors will test the proposed method for interpretation of several tens of experiments on thermally stimulated rock failure. Results of this testing will be presented in the future works.

## Conclusions

Authors examine the problem of estimating the parameter *b* for energy distribution of thermoacoustic emission events based on the amplitude distribution of its impulses.

The scheme of the laboratory setup for the study of thermally stimulated rock failure with registration of TAE impulses by a single sensor was given. The effect of factors associated with the elastic wave propagation on the impulse energy was analyzed. It is shown that the absorption of elastic waves in a heated sample has the greatest effect; spreading of the waves can be taken into account as a linear addition to the specific absorption coefficient; other factors under certain assumptions can be neglected.

The one and two sub-function distribution laws of TAE events are considered. It is theoretically shown that the same value of *b* of the recorded amplitude distribution of impulses and initial event distribution is observed only in the case of the one sub-function law when *b* is constant throughout the entire energy range of TAE events. In such situation it can be assumed that one characteristic generation mechanism of events prevails over the entire volume of the sample or, that in order to clarify the issue of the AE mechanisms, in addition to the amplitude distribution of impulses other data will be required. In the case of different values of *b* in the energy range (two sub-function law) attenuation of the elastic waves in the sample distorts the original distribution.

The method of analyzing the distribution of registered TAE impulses in several amplitude subranges is proposed. It allows to understand the nature of the distribution law of events determining whether it is a one sub-function or more complex, and also to estimate the "true" value of the *b-value* parameter.

## Acknowledgements

## References

AE Test. Site about acoustic emission control method and package AE Workbench. Komarov A. 2017. URL: http://www.aetest.ru.

Amitrano D. Variability in the power-law distributions of rupture events, How and why does b-value change. *Eur. Phys. J. Special Topics,* 2012, vol. 205, pp. 199-215.

Damaskinskaya E.E., Panteleev I.A., Kadomtsev A.G., Naimark O.B. Effect of the state of internal boundaries on granite fracture nature under quasi-static compression, *Physics of the Solid State*, 2017, vol. 59, iss. 5, pp. 944-954.

Damaskinskaya E.E., Panteleev I.A., Gafurova D.R., Frolov D.I. Structure of a deformed inhomogeneous material on the data of acoustic emission and X-ray computer microtomography, *Phys. Solid State*, 2018, vol. 60, iss. 7, pp. 1363-1367.

Davies R.M. Stress waves in solids. Cambridge University Press, 1961.

Kaznacheev P.A., Majbuk Z.-Yu.Ya., Ponomarev A.V., Smirnov V.B., Bondarenko N.B. The laboratory study of thermally stimulated failure of rocks, in *Triggernye effekty v geosistemakh: materialy IV Vserossijskoj konferentsii s mezhdunarodnym uchastiem*. (Trigger effects in geosystems: Materials of IV all-russian conference with international participation), Moscow: GEOS, 2017, pp. 163-171.

Markov E.A. Evaluation of informativeness of structure of acoustic emission signals from microcracks in thin-walled objects: PhD thesis. Moscow, MISIS, 2007.

Okal E.A., Romanowicz B. On the variation of b-values with earthquake size, *Physics of the Earth and Planetary Interiors,* 1994, vol. 87, pp. 55-76.

Pisarenko V.F., Rodkin M.V. The estimation of probability of extreme events for small samples, *Pure Appl. Geophys*, 2017, vol. 174, pp. 1547-1560.

Ponomarev A.V., Zavyalov A.D., Smirnov V.B., Lockner D.A. Physical modeling of the formation and evolution of seismically active fault zones, *Tectonophysics*, 1997, vol. 277, pp. 57-81.

Shkuratnik V.L., Voznesenskij A.S., Vinnikov V.A., *Termostimulirovannaya akusticheskaya emissiya v geomaterialakh* (Thermally stimulated acoustic emission in geomaterials), Moscow: Gornaya kniga, 2015.

Sych T.V. Improvement of acoustic emission control technology based on finite element analysis of acoustic path: PhD thesis. Novosibirsk, STU, 2016.

Vasin R.N., Nikitin A.N., Lokajicek T., Rudaev V. Acoustic emission of quasi-isotropic rock samples initiated by temperature gradients. *Izv. Phys. Solid Earth*, 2006, vol. 42, no. 10, pp. 815-823.

Vettegren V.I., Bashkarev A.Y., Morozov G.I., Lebedev A.A., Nefed'ev E.Yu., Kryuchkov M.A. Influence of structural interfaces on the statistics of corrosion microcracks, *Phys. Solid State*, 2005, vol. 47, iss. 10, pp. 1869-1871.

Vettegren, V.I., Kuksenko, V.S., Tomilin, N.G., Kryuchkov M.A. Statistics of microcracks in heterogeneous materials (granites), *Phys. Solid State*, 2004, vol. 46, iss. 10, pp. 1854-1858.